

Stimulus-Contrast-Induced Biases in Activation Order Reveal Interaction Between V1/V2 and Human MT+

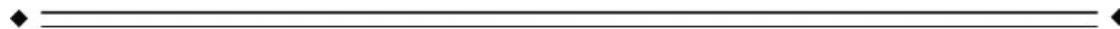
Masaki Maruyama,* Daniel D. Palomo, and Andreas A. Ioannides

Laboratory for Human Brain Dynamics, RIKEN Brain Science Institute, 2-1 Hirosawa, Wakoshi, Saitama 351-0198, Japan



Abstract: The luminance contrast of a visual stimulus is known to modulate the response properties of areas V1 and the human MT complex (hMT+), but has not been shown to modulate interactions between these two areas. We examined the direction of information transfer between V1/V2 and hMT+ at different stimulus contrasts by measuring magnetoencephalographic (MEG) responses to moving and stationary stimuli presented centrally or peripherally. To determine the direction of information flow, the different response latencies among stimuli and hemispheres in V1/V2 was compared with those of hMT+. At *high* contrast, responses to stimulus motion and position began in V1/V2, and were followed in hMT+ with a delay between 34 and 55 ms. However, at *low* contrast, lateralized responses in hMT+ came first, with those in V1/V2 lagging with a delay of 27 ms. Also, at high contrast, stationary stimuli produced greater responses than motion stimuli in V1/V2, while the reverse was true in hMT+, whose response lagged behind the initial response in V1/V2. The same activation order was found using Mutual Information Analysis of the response variances for each condition. Here, the response variances in hMT+ mimicked and trailed those of V1/V2 at high contrast, whereas the reverse was true at low contrast. Such consistent interactions found using two different methodologies strongly supports a processing link between these two areas. The results also suggest that feedback from hMT+ for low-contrast stimuli compensates for unresolved processing in V1/V2 when the input of a visual image is weak. *Hum Brain Mapp* 30:147–162, 2009. © 2007 Wiley-Liss, Inc.

Key words: functional connectivity; visual motion; magnetoencephalography; mutual information analysis; visual field asymmetry; lateralization



INTRODUCTION

The parieto-temporo-occipital area known as the human medial temporal complex (hMT+) responds more strongly to moving than stationary patterns [Cheng et al., 1995; Dumoulin et al., 2000; Huk et al., 2002; Sunaert et al., 1999; Tootell et al., 1995; Zeki et al., 1991]. MT in monkeys has direct anatomical connections with the primary visual area (V1) [Maunsell and van Essen, 1983], and their feed-forward and feedback processing have been well explored [for review, see Born and Bradley, 2005]. For example, Sil-lito and colleagues have recognized the role of feedback circuits from MT to V1 in their ability to “shape” bottom-

Additional Supporting Information may be found in the online version of this article.

*Correspondence to: Dr. Masaki Maruyama, Laboratory for Human Brain Dynamics, RIKEN Brain Science Institute, 2-1 Hirosawa, Wakoshi, Saitama 351-0198, Japan. E-mail: mmasaki@brain.riken.jp

Received for publication 4 May 2007; Revised 30 July 2007; Accepted 31 August 2007

DOI: 10.1002/hbm.20495

Published online 27 November 2007 in Wiley InterScience (www.interscience.wiley.com).

up inputs from V1, similar to the reciprocal connections V1 maintains with LGN [Sillito et al., 2006]. V1 is also known to send direction-selective signals [Movshon and Newsome, 1996] that increase the direction selectivity of MT neurons [Girard et al., 1992]. Conversely, MT may reinforce this process by selecting coherent inputs from V1 through feedback connections. This would be particularly beneficial when input signals from V1 are weak due to conditions such as low contrast. Under such conditions, we hypothesized that MT may attempt to compensate for weak V1 signals, an effect that should be discernable by a greater or earlier activation relative to V1, as compared with conditions in which the stimulus was more salient.

There exist models of visual processing which suggest that local information detected in V1 is further processed in MT to reduce noise [Qian and Andersen, 1994; Snowden et al., 1991], and to derive structure from motion [Andersen and Bradley, 1998]. In the absence of this forward pathway, based on the recording of V1 activity under conditions of MT inactivation, Hupe et al. [1998] concluded that the feedback from MT serves to differentiate figure from ground in V1. In humans, transcranial magnetic stimulation (TMS) has demonstrated the importance of feedback from hMT+ to V1 (a process taking from 5 to 50 ms) in visual motion awareness [Pascual-Leone and Walsh, 2001; Silvanto et al., 2005a]. Another TMS study revealed that critical periods for awareness in V1 exist before (40–60 ms from stimulus onset) and after (80–100 ms) a critical period in hMT+ (60–80 ms), but did not overlap [Silvanto et al., 2005b], implying feed-forward and feedback dynamics between these areas. Together, these findings suggest that MT plays an important role in integrating and interpreting motion signals generated by V1, and may be additionally taxed when incoming motion signals are weak.

Despite the progress in understanding the interaction between V1 and hMT+, its dependence on stimulus properties is poorly understood. However, it is known that neurons in all areas of V1 and MT modify their response properties at low luminance contrast to increase their sensitivity to weak signals [Kapadia et al., 1999; Levitt and Lund, 1997; Pack et al., 2005; Sceniak et al., 1999]. In humans, as stimulus contrast decreases, activation in V1 dramatically drops, but hMT+'s response is largely unaffected [Tootell et al., 1995]. Whether the interaction between V1 and MT is also affected by luminance contrast is a key unanswered question. A finding of a contrast-dependent effect would be indicative of MT's active role in enhancing weak bottom-up motion signals. Accordingly, if MT reinforces motion signals through feedback, its role should be more apparent when the input signal is weak, as in the case of low-contrast motion stimuli.

In the current study, we applied the term *activation shift* when a delayed association was found between the responses of these two areas. Such an effect is indicative of information transfer. Thus, the current study aimed to detect a possible activation shift between V1/V2 and hMT+

induced by differences in stimulus contrast. The positive and negative response delays in V1/V2 linked to hMT+ are a key indicator of this direction. In our investigations, we recorded neural activities at high temporal resolution using MEG.

Previous studies have often compared the onset latencies of the initial responses between brain areas to elucidate signal pathways [Foxe and Simpson, 2002; Inui and Kakigi, 2006; Schmolesky et al., 1998]. The difference in our approach is that we examined the latencies for the peaks obtained from *stimulus condition comparisons*. By using several dimensions of stimulus modulations, we created an activation "signature" whose shift could be tracked from one area to another. Thus, in the current study, we provide evidence for a direct interaction between V1/V2 and hMT+ by examining *the shift of activation dependence* on stimulus conditions.

We examined the peak latencies of response variances resulting from the varying of conditions such as stimulus motion and location, as well as the response variances of stimulus-induced lateralization effects. We interpreted the presence of a significant motion effect in V1/V2 before a similar effect in hMT+ as an indication of a stimulus-dependent activation that propagated from V1/V2 to hMT+. Accordingly, we examined the shift in these dependencies for the *averaged response* across trials in each stimulus condition.

We also examined the activation shift for *response variances* within each stimulus condition. In this case, our approach was to use Mutual Information Analysis (MI) [Shannon, 1948] to detect associations in the response variances. For example, when the response variance in V1/V2 was found to be associated with a later response variance in hMT+, we considered this an activation shift from V1/V2 to hMT+ with a positive delay.

MATERIALS AND METHODS

Subjects

Eight, healthy, right-handed drug-free men participated in the experiment. Right-handedness was determined by the 10-item Edinburgh handedness inventory [Oldfield, 1971]. Their ages ranged from 25 to 36 years, with a mean age of 30 years. All experimental procedures were undertaken with the understanding and written consent of each subject, and conformed to The Code of Ethics of the World Medical Association (Declaration of Helsinki), and were approved by the RIKEN Ethics Committee.

Visual Stimuli and Task

Each subject was comfortably seated inside a magnetically shielded room ($3 \times 4 \times 2.4 \text{ m}^3$, NKK, Japan). Visual stimuli were back-projected on a screen ($39 \times 29 \text{ deg}$) by a digital-light-processing projector (HL8000Dsx+, NEC, Tokyo, Japan) placed outside the shielded room. The distance

from the subject to the screen was 58 cm. The projector had a frame rate of 96 Hz and a spatial resolution of 0.038 deg per pixel. Given that screen luminance decays with eccentricity, the uncorrected intensity of central stimuli tends to be greater than peripheral stimuli (a difference greater than fourfold in our experimental environment). In addition, the luminance may vary among peripheral areas (e.g., 50% difference at maximum). To correct for these conditions, first, we strongly reduced central luminance with two central neutral-density filters (PRO ND8, Kenko, Tokyo, Japan). The remaining luminance difference was precisely corrected by controlling the luminance gain of the projector at a spatial resolution of 2 deg with a linear interpolation map uploaded to the projector. The luminance was adjusted for a viewing range of 29×18 deg from the subject's viewpoint. The resulting minimum-to-maximum luminance ratio during the experiments ranged from 1.03 to 1.12, with an average of 1.08. When compared with other MEG studies in which a simple screen was used for stimulus presentation, we believe our improved method afforded more precise examination of visual field asymmetries.

A random dot pattern was presented peripherally to one of: top-right, top-left, bottom-right, or bottom-left locations (eccentricity, 8 deg; pattern size, 8 deg in diameter; dot size, 0.15 deg; density, 5 dots/deg²), or centrally, (pattern size, 2 deg in diameter; dot size, 0.038 deg; density, 80 dots/deg²) [see Fig. 1(A)]. The size and eccentricity of the peripheral stimuli were chosen so as to control for the cortical magnification factor relative to the central stimuli [Rovamo and Virsu, 1979]. Dots were either stationary or expanding at 15 deg/s in the periphery, and 3.8 deg/s in the central areas. We manipulated the dot lifetime for the motion stimuli to keep the dot distribution uniform. Each dot was presented for 200 ms, and then disappeared and randomly reappeared at a new location in an asynchronous manner. Low-contrast (0.2 by the Michelson definition) and high-contrast (0.8) stimuli were created by setting the dot luminance to 10.5 and 63 cd/m² respectively, and the background luminance to 7 cd/m². The shielded room was dark, with the stimuli as the only source of light. The stimuli were generated by Presentation software (Neurobehavioral systems, Version 0.80, Albany, CA). The image signal from the stimulus computer was synchronized with the frame transition of the projector.

The subjects were instructed to fixate a black dot (0.076 deg in size; luminance 0.08 cd/m²) at the center of the screen. To maintain arousal, the subjects were asked to quickly lift the index finger of their right hand from an optic button when the color of the fixation square changed to red [Fig. 1(B)]. This color change was rare and unpredictable. Both the random dot patterns and the red fixation square were presented for 300 ms with an inter-stimulus interval of 700 ± 100 ms. In each run, each stimulus condition (5 locations; motion/static; 2 contrasts) was presented 15 times (e.g., in 15 trials) and the color of the fixation

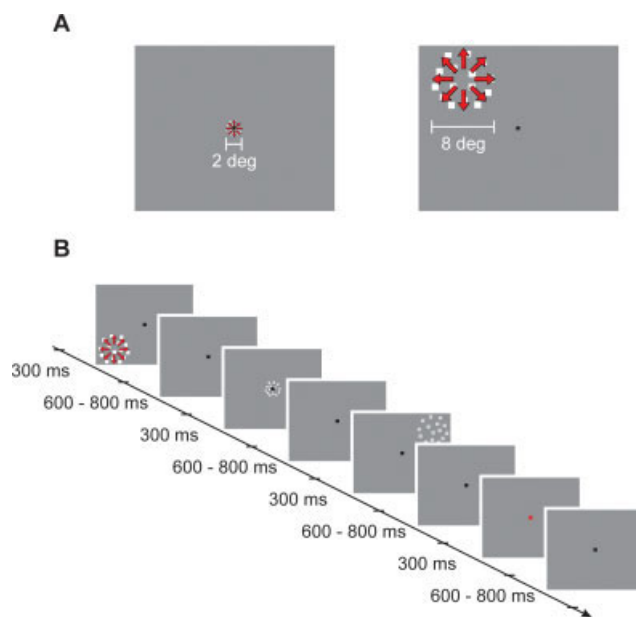


Figure 1.

(A) Random dot patterns were presented either centrally or to one of four quadrant areas. In motion stimuli, dots moved outward from the center of the pattern (schematic red arrows). (B) Representation of the stimulus sequence. The subjects were instructed to fixate the central square and to release a button when the color of the fixation square changed from black to red.

square changed 1, 2, or 3 times at random points during the run. All subjects performed 10 such runs.

Data Acquisition and Preprocessing

Magnetic field responses were measured with a whole-head MEG system (Omega, CTF Systems, Vancouver, Canada). On the inner, lower surface of the helmet-shaped dewar, 151 primary sensors are uniformly distributed with a separation of 3.1 cm. Each sensor is a first-order axial gradiometer consisting of two coils with a diameter of 2 cm and axial separation of 5 cm. In addition, 29 reference sensors (9 magnetometers and 20 gradiometers) are placed above the primary sensors to construct a high-order gradiometer, which effectively eliminates environmental noise [Vrba and Robinson, 2001].

The subject's eye movement artifacts and heart function were simultaneously measured with a horizontal electrooculogram (EOG) (1 cm lateral to the left and right outer canthus of the eyes), a vertical EOG (1 cm above and below the left eye), limb electrocardiogram (ECG) (on the left and right wrists and the left ankle), and lead V2 ECG (at the height of the nipple 2 cm left of the midline) for off-line noise reduction. In addition, we recorded the signal from a photodiode attached to the screen frame on the side opposite the subjects to measure the actual stimulus

timing upon which the analysis was based. MEG, EOG and ECG data were recorded continuously during each run. The recording time of each run was 302 s on average. The subject's head location was recorded at the beginning and the end of each run, using three coils attached to the scalp—one close to the nasion, and two close to the left and right preauricular points. When the head movement during a run exceeded 6 mm, the recording of the run was repeated.

The signals were low-pass filtered below 200 Hz (second-order), and sampled at 625 Hz. The environmental noise was removed from the MEG signals by using the reference channels to form a third gradient of the magnetic field, as described earlier. After DC-offset removal, the signals were band-pass filtered below 200 Hz and above 3 Hz (fourth order), and notch-filtered to eliminate power line noise and harmonics at 50, 100, 150, and 200 Hz (second-order, half-width 3 Hz) using CTF software (designed for filtering and constructing high-order gradiometers, etc.). We extracted trials from each run, between 300 ms before and 600 ms after the onset of the stimulus. The EOG signal was visually inspected, and any trials that contained blinks or saccadic eye movements around the stimulus presentation (-100 to $+300$ ms from the onset) were discarded. For all subjects, more than 10 trials remained for each run and stimulus condition (14.5 trials on average). Independent Component Analysis (ICA) was then applied, and components correlated to the EOG and ECG signals were eliminated to remove the subjects' heart-beat and eye-blink artifacts [Jahn et al., 1999]. The preprocessed signals were averaged separately for each stimulus condition and each run with respect to the stimulus onset as detected by the signal from the photodiode, thus giving 200 averaged trials (20 conditions \times 10 runs).

Coregistration of MEG and MRI

Magnetic resonance images (MRI) were taken with either a 1.5 T Magnetom Symphony (Siemens, Erlangen, Germany) or ExcelArt (Toshiba, Tochigi, Japan) MRI machine covering the whole head. In both cases, 256 slices of T1-weighted sagittal images were collected with 1 mm spacing. Each slice consisted of a 256×256 matrix with a pixel size of 1×1 mm². The head contour was extracted with Brain Voyager QX (Brain Innovation, Maastricht, The Netherlands). The subjects' head shape and the position of the head-localization coils relative to the head were measured with a 3D digitizer (Fastrak, Polhemus, VT) and a 3D camera system (VIVID 700, Konica Minolta Holdings, Tokyo, Japan). The position of each head-localization coil relative to the others and to the primary sensors was measured by activating the coils electronically via the MEG system. The relative positions of the coils were matched to the digitized coil positions. The digitized head shape was fitted onto the MRI-extracted contour with Rapid Form (INUS Technology, Seoul, Korea) and dedicated in-house software [Hironaga et al., 2002]. The average distance

between the digitized head shape and the MRI contour was less than 1.5 mm in every subject.

Source Analysis

We extracted tomographic estimates of activity from the averaged MEG signals using Magnetic Field Tomography (MFT) [Ioannides, 1990; Ioannides, 1994]. The classical minimum norm approach tends to estimate source current more closely to the surface of the brain than veridical by using a linear expansion of the sensitivity profile of the sensors. In contrast, MFT relies on a non-linear algorithm that mitigates this tendency using an a priori probability weight that compensates for the greater sensitivity to superficial rather than deep sources. The MFT algorithm also uses a regularization parameter [Ioannides et al., 1990] to resolve the conflicting requirements of high spatial accuracy and insensitivity to noise. The standard deviation of the a priori probability distribution relative to that of the MEG data is constrained to a finite value, which excludes results with physiologically implausibly large current amplitude. The use of an a priori probability weight and regularization renormalizes the current density, thus MFT output results in arbitrary units (au). Although the renormalization depends on the level of noise, it does not affect relative changes in time at different brain locations or across different experimental conditions.

Four separate MFT computations were performed, in each case using partially overlapping hemispheric source spaces ($17 \times 17 \times 11$ grid points each) which completely covered the left, right, back, and top (superior parts of the brain) [Ioannides, 2002]. Each MFT computation uses a spherical conductor model for the conductivity of head [Grynspan and Geselowitz, 1973], with the center of the conducting sphere in each case chosen to fit the inner surface of the skull in the appropriate hemisphere. Source currents were allowed only within the appropriate source space, i.e., the brain area of the corresponding MFT hemisphere (left, right, back and top). MFT was performed separately for each source space, after choosing 90 MEG sensors from the corresponding side. The solutions from all four source spaces were combined into a *single, large source space* which covered the whole brain, using the sensitivity-profile-modified current density values of the sensors from nearby points in the individual source spaces. The results were stored at a resolution of 9–12 mm depending on the size of subject's head. The algorithmic steps and mathematical details of MFT can be found elsewhere [Ioannides, 1995; Taylor et al., 1999].

Definition of Regions of Interest

The MEG signal is generated by electrical neuronal activity which at the macroscopic level is represented by the current density vector. We defined regions of interest (ROIs) in V1/V2 and hMT+, at foci showing a strong current density consistent in amplitude and direction across

runs, as quantified by an estimator of signal-to-noise ratio [SNR; Laskaris and Ioannides, 2002]. To separate V1/V2 from hMT+, we chose stimuli expected to isolate either area. Thus, we defined the V1/V2 ROIs contralateral to stimulus presentation by defining SNR as the power of the responses (defined as the averaged square of the responses over all runs), normalized by the power of the response variance for all high-contrast stimulus conditions. On the other hand, hMT+ ROIs were defined separately for each hemisphere at both high and low contrasts, defining signal power by contrasting the responses of motion stimuli to stationary stimuli. Given the naturally high SNR in V1/V2, our ROI definition there was set based on a starting criterion SNR of 2, whereas with the naturally weaker SNR in hMT+, we were forced to choose a lower starting cut-off level of 1 in defining this ROI.

In defining the V1/V2 ROI, we took advantage of the fact that V1/V2 is selective for high-contrast stimuli. We therefore presented high-contrast stationary random dot fields to each visual quadrant as well as centrally. We then restricted our search area to the occipital lobe based on the co-registered MRI image, and looked for foci of activation exceeding a given SNR threshold. The threshold was initially set to 2.0 and gradually dropped as low as 1.0 until at least one region met the criterion. Next, we ascertained that our identified foci exhibited the expected retinotopic arrangement. Indeed, for stimuli presented to the upper and lower visual hemifields we obtained threshold activations below and above the calcarine sulcus (respectively) in contralateral cerebral hemispheres, and for centrally presented stimuli we found a focus in the occipital operculum.

To localize hMT+, we employed a contrast between moving and stationary stimuli known to favor selective activation in hMT+ [Zeki et al., 1991]. Low contrast stimuli were included with high contrast stimuli to improve localization accuracy since they are also known to elicit hMT+ activation [Tootell et al., 1995]. We limited our search area to the temporo-parieto-occipital area surrounding the junction of the inferior temporal sulcus (ITS) with its upper limb, its posterior continuation, and the lateral occipital sulcus (LOS). hMT+ has been reliably colocalized to these sulci [Dumoulin et al., 2000]. We then sought foci satisfying an SNR criterion based on the difference between activations to motion and stationary stimuli. The threshold was initially set to 1.0 and gradually dropped as low as .1 until at least one region met the criterion. The resulting foci failed to show significant differences in location under ANOVA. Therefore, we defined the center of each ROI as the average of the SNR-weighted foci among all stimulus conditions. For further details of the ROI definition, please refer to the Supplementary Materials.

In the following analyses of shifts in neural activation, we used the component of the current density vector projected onto the averaged direction across runs, separately for each stimulus condition at each time slice. This component increases when current flows strongly in a common direction across the runs.

Statistical Analysis of Activation Shift Based on Averaged Responses

The effects of the stimulus conditions as well as lateralization effects were tested at each contrast and time-slice in the period from -100 to 300 ms from stimulus onset. The prestimulus baseline was determined separately for each stimulus and each ROI by averaging the response for 100 ms before the onset. We first applied Analysis of Variance (a grand ANOVA) across the subjects in search of general effects and their latencies. Given the high probability of Type 1 errors, we judged the effects to be significant only when they continuously satisfied a Type 1 error criterion of $P < 0.01$ for at least 6.4 ms, or $P < 0.001$ for at least 3.2 ms. Use of this criterion eliminated spurious effects prior to stimulus onset. We then applied individual ANOVAs (at $P < 0.05$) for each subject in order to compare the latency of the general effects between V1/V2 and hMT+ in each subject. The factors Run and Subject were always treated as random factors. When interactions were significant, post hoc multiple comparisons were performed using Scheffe's procedure. All statistical tests were performed using SPSS software (SPSS, Chicago, IL).

The latency of each effect was compared between the areas in order to estimate shifts in the averaged response. The latency of each area was defined as the time point of the peak F -value (F_{peak}), and was used to test the significance of each effect in the individual ANOVAs. (The F -value is a measure of the separation of two or more population distributions.) The F -value chosen thus represented the power of the response variance between the stimulus conditions (e.g., between motion and stationary stimuli), or between hemispheres, normalized by the power of the response variance in each stimulus condition. The F_{peak} of individual ANOVAs was detected within a range between -50 and $+50$ ms with respect to the latency of a significant effect in the grand ANOVA. Four grand ANOVAs examined the effects of central and peripheral stimuli, and V1/V2 and hMT+ responses, using the same factors as the individual ANOVAs but replacing run by subject (Please refer to Table I). For further details on the definition of F -value, please refer to the Supplementary Materials.

Mutual Information Analysis of Activation Shift Based on Response Variances

In this analysis, we used the MFT solutions to examine the shift in the regional *response variances* among the runs in each stimulus condition and in each ROI. We quantified the association in the response variances between the two areas (V1/V2 and hMT+) using MI analysis, which unlike the often-used correlation coefficient, is sensitive to both linear and nonlinear association. We termed this measure the *relatedness* between the two areas. MI provides an index of the relatedness between two separately measured quantities. In effect, it gives the probability that one such measure can be predicted from the other (see Appendix

TABLE I. Factors considered in the individual ANOVAs

ROI	Visual field	Factor
V1/V2	Center	Motion, run
	Peripheral	Motion, vertical position, hemisphere, run
hMT+	Center	Motion, hemisphere, run
	Peripheral	Motion, vertical position, horizontal position, hemisphere, run

The individual ANOVAs were applied separately for each contrast. Run is always treated as a random factor.

for details). The delay in relatedness between these areas was used as our second measure of activation shift.

MI was calculated between V1/V2 and left hMT+, and between V1/V2 and right hMT+ separately for each stimulus condition and for each subject. The value of MI increases as the degree of the relatedness increases. High MI between the V1/V2 response at a latency t and the hMT+ response at $t + \tau$ [$MI_{V1 \rightarrow MT}(t, \tau)$, $\tau > 0$] implies a shift in activation from V1/V2 to hMT+. In contrast, high MI between the hMT+ response at a latency t and the V1/V2 response at $t + \tau$ [$MI_{MT \rightarrow V1}(t, \tau)$, $\tau > 0$] implies a shift of activation in the reverse direction.

The value of MI was analyzed statistically over all subjects by performing an ANOVA at each latency and delay. In addition to the effects of stimulus condition, we tested the effect of order of latency between V1/V2 and hMT+ by contrasting $MI_{V1 \rightarrow MT}(t, \tau)$ with $MI_{MT \rightarrow V1}(t, \tau)$. We deemed the effects significant only when they continuously satisfied a criterion of $P < 0.05$ for more than 24 ms, a period chosen so that no significant effect of stimulus condition could be obtained before stimulus onset. Significant interactions were further analyzed by Scheffe's multiple comparisons test.

RESULTS

Overview

In the current study, evoked magnetic fields were detectable at both low and high contrast conditions [Fig. 2]. A grand ANOVA across the subjects demonstrated significant effects of stimulus vertical position and motion at high contrast, and lateralized activation at low contrast for both V1/V2 and hMT+ [Figs. 3 and 4]. Individual comparisons of latency at high contrast revealed significant effects of vertical position and motion which began in V1/V2 and followed in hMT+. However, at low contrast, the lateralized activation in V1/V2 lagged behind hMT+ [Figs. 5 and 6]. MI analysis between V1/V2 and hMT+ revealed that V1/V2 always led in significant MI relatedness (as defined in Methods) at high contrast, but at low contrast, hMT+ more often led V1/V2 in significant relatedness [Figs. 7 and 8]. Estimated directions of activation transfer are summarized in Figure 9.

Magnetic Field Response and Regions of Interest

Figure 2 shows examples of MEG signal timecourses [Fig. 2(A,B)] and SNR tomographic displays derived from MFT estimates of the current density vector for one subject [Fig. 2 (C,D)]. The butterfly plots show the averaged field in one run for a high-contrast stimulus [Fig. 2(A)], and for a low-contrast stimulus [Fig. 2(B)], each averaged over 14 trials. In both contrast conditions, the evoked response to the stimulus was distinguishable from background activities, but high-contrast stimuli generally evoked stronger responses than low-contrast stimuli. The plots on the right of the two butterfly plots show the signal topography at the latencies marked by the vertical dashed line in the butterfly plots. The main panels in the last row [Fig. 2(C,D)] show SNR contour plots at the latencies corresponding to the signal topographies [Fig. 2(A,B), respectively] and marked by the dashed vertical lines in the butterfly plots. The SNR is computed independently for each source space point from the instantaneous MFT estimate for the current density vector across the 10 runs of one condition. The SNR plots show the results for V1/V2 at 44 ms [Fig. 2(C)] and for hMT+ at 150 ms [Fig. 2(D)]. In each case, the whole brain and a zoomed image in the main panel show the SNR contours (dashed yellow lines) and the locus of the very first area satisfying a criterion of 2 for V1/V2, and 1 for hMT+ (red regions bounded by solid yellow lines). The zoomed images on the right of each main panel show the region of first high SNR again, together with the main sulci in each area—the calcarine for V1/V2 and the LOS and the anterior limb of the ITS (ALITS) for hMT+.

ROIs were defined based on SNR foci such as the ones shown in Figure 2(C,D) as detailed in the Supplementary Materials. The ROI positions were converted into Talairach coordinates [Talairach and Tournoux, 1988], and their averages and SDs are summarized in Table II. Our hMT+ locations agreed with previous functional MRI (fMRI) studies [Dumoulin et al., 2000; Hasnain et al., 1998; Tootell et al., 1995], and with a positron emission topography (PET) study [Zeki et al., 1991] (lateral: 38–47, posterior: 62–76, superior: –1 to 8). The nearest sulcal landmarks to the individual ROI centers are listed in Table II.

Statistical Results Based on Averaged Responses

Grand-averaged responses for the central stimuli are plotted in Figure 3. At high contrast (left panels), hMT+ exhibited a higher response to the motion stimuli [solid lines in Fig. 3(A)] than for the stationary stimuli (dashed lines). A grand ANOVA identified a significant motion effect on hMT+ response in both hemispheres (in the range of 194.4–205.6 ms, $P < 0.01$), followed by the effect in the left hemisphere (228.0–232.8 ms, $P < 0.01$). At high contrast, [Fig. 3(B)] the response of V1/V2 to the motion stimuli was significantly lower compared with the stationary stimuli (116.0–130.4 ms at $P < 0.01$ and 159.2–160.8 ms

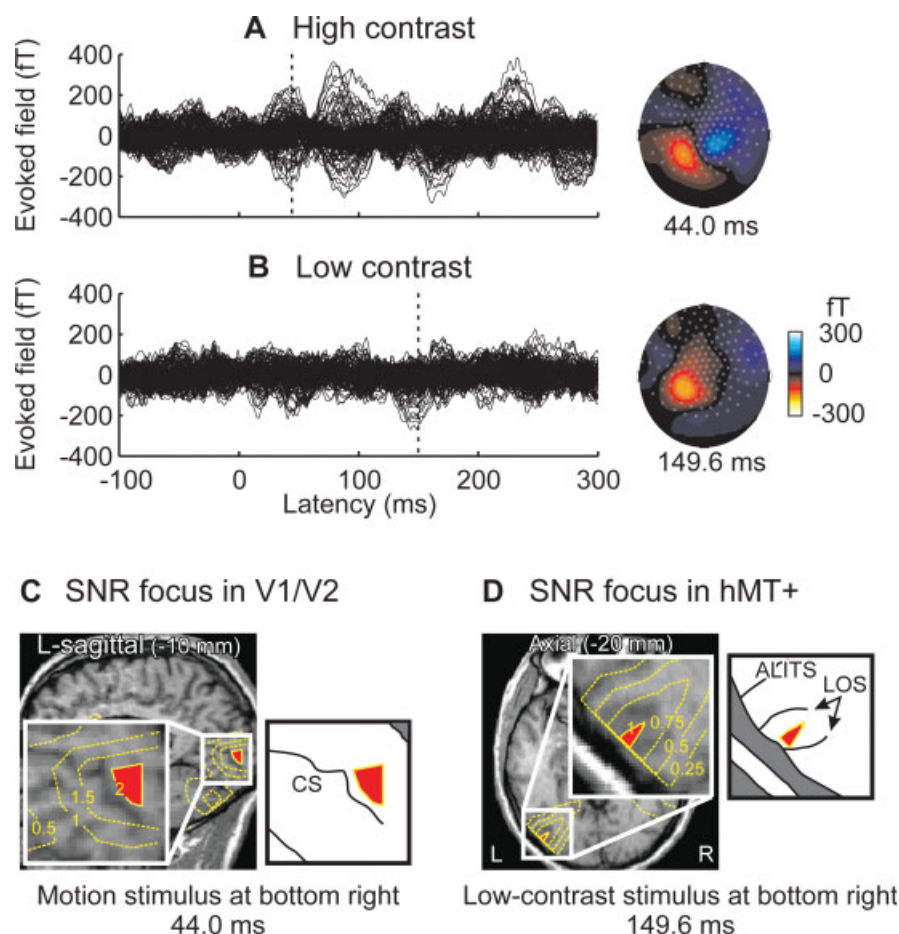


Figure 2.

(A) Butterfly plots of individual sensor fields averaged over 14 trials in one run for a high-contrast moving stimulus presented to the bottom-right visual field. The distributions of the magnetic field are given on the right contour maps, at the latency marked by the dashed line. fT, femtoTesla. (B) Low-contrast stimulus producing clearly diminished activations. (C) SNR contour plot derived from the MFT estimates of the current density vector for motion stimuli at high contrast. The red region indi-

cates the brain area which is first to satisfy an SNR criterion of 2 in V1/V2. CS, Calcarine sulcus. (D) SNR contour plot as in (C) for low contrast stimuli presented to the bottom right. The red region indicates the first brain area satisfying an SNR criterion of 1 in hMT+ at low contrast. LOS, lateral occipital sulcus; ALITS, ascending limb of the inferior temporal sulcus. The stimuli were presented in the lower-right visual field.

at $P < 0.001$). At low contrast, no significant difference was found (right panels).

Figure 4(A) shows grand-averaged responses to the peripheral stimuli presented to the bottom-right visual field. Similar time-courses of grand-averaged responses were obtained for the other peripheral locations. With the peripheral stimulus, the response in hMT+ was higher for motion than stationary stimuli at both contrasts whereas in V1/V2 it was higher for stationary than motion stimuli at high contrast.

Grand ANOVAs across the peripheral stimuli at each contrast found significant effects for stimulus motion (hMT+: 135.2–140 ms and 210.4–228.0 ms, $P < 0.01$; V1/V2: 101.6–106.4 ms, $P < 0.01$) and vertical position (hMT+:

124.0–125.6 ms, $P < 0.001$; V1/V2: 60.0–143.2 ms, $P < 0.01$) at high contrast, and a significant lateralization effect at low contrast (hMT+: 108.0–119.2 ms, $P < 0.01$; V1/V2: 114.4–119.2 ms, $P < 0.01$) in both V1/V2 and hMT+. In Figure 4(B), we plot the time courses of response differences. For example, the red lines represent the difference between the stationary and motion stimuli averaged over all quadrants, for stimuli presented contralaterally (solid lines) or ipsilaterally (dotted lines) to the activated region. The blue line represents the difference between responses to top versus bottom stimuli. The difference between the hemispheres is represented by the green line.

A significant motion effect in hMT+ was obtained in the hemisphere contralateral to stimulus location [bold red

TABLE II. Talairach coordinates and nearest sulci for the ROI centers in V1/V2 and hMT+

Subject	V1/V2				
	Stimulus position				
	Bottom left	Bottom right	Center	Top left	Top right
1	10, -85, 5, Above RCS	-12, -84, 13, Above LCS	-1, -81, -3, RCS	3, -77, 3, Below RCS	-11, -70, 9, Below LCS
2	10, -77, 7, RCS	-9, -72, 10, LCS	-5, -90, -9, LCS	10, -78, 0, Below RCS	1, -68, 4, Below LCS
3	14, -62, 5, RCS	-9, -85, -3, Above LCS	-4, -86, -9, Above LCS	9, -65, 8, RCS	-9, -65, 0, LCS
4	15, -76, 9, RCS	-8, -79, 1, LCS	15, -81, -1, RCS	14, -60, -9, Below RCS	-2, -78, -5, LCS
5	0, -77, 8, R-paraCS	-10, -73, 11, LCS	-9, -85, -7, Above LCS	0, -73, 1, RCS	-15, -73, 4, LCS
6	15, -85, 0, Above RCS	-10, -86, -1, Above LCS	2, -83, -5, RCS	14, -79, -4, RCS	-10, -80, -4, Below LCS
7	13, -79, 4, RCS	-9, -89, -1, Above LCS	2, -83, -13, L-retroCS	13, -72, -1, Below RCS	2, -73, -7, Below LCS
8	10, -90, 5, Above RCS	-3, -92, 2, Above LCS	1, -88, 3, Above LCS	10, -68, 5, Below RCS	-8, -68, 8, LCS
Avg. (SD)	10, -79, 5, (5, 9, 3)	-9, -83, 3, (3, 7, 6)	0, -85, -6, (7, 5, 6)	9, -72, 1, (5, 9, 4)	-7, -72, 1, (6, 5, 7)
Subject	Left hMT+		Right hMT+		
1	-40, -70, 6, LOS		39, -67, 6, ALITS		
2	-36, -70, 8, Anterior LOS		38, -69, 10, Anterior LOS		
3	-39, -71, -4, Anterior LOS		37, -61, 7, ALITS		
4	-38, -65, 4, Anterior LOS		39, -64, 6, ALITS		
5	-47, -73, 11, ALITS		39, -59, 8, ALITS		
6	-42, -67, -7, ALITS		42, -68, 3, ALITS		
7	-38, -66, 1, ALITS		38, -66, 0, ALITS		
8	-42, -70, 0, ALITS		45, -68, 6, ALITS		
Avg. (SD)	-40, -69, 2, (6, 7, 7)		39, -65, 5, (5, 7, 6)		

ROI centers for V1/V2 represent the average of motion and stationary stimuli. ROI centers for hMT+ represent the average of high and low contrast stimuli and stimulus positions. ROI volumes were determined using a spherical region of weight decay with a radius of 4.6 mm for V1/V2 and 14 mm for hMT+ (see Supplementary Fig. 1 for more details).

X(+), right; Y(+), anterior; Z(+), dorsal; RCS, right calcarine sulcus; LCS: left calcarine sulcus; R-paraCS: right para-calcarine sulcus; LOS: lateral occipital sulcus; ALITS: ascending limb of the inferior temporal sulcus.

asterisks in Fig. 4(B)], followed by a bilateral motion effect (paired bold and thin red asterisks). Significant lateralization effects are marked by the green asterisks. The differential responses in V1/V2 to top and bottom stimuli exhibited two peaks at high contrast (blue asterisks). Hereafter, we call these *early period* and *middle period* effects, respectively.

Thus, we have presented the significant effects in V1/V2 and hMT+ for all subjects combined. In general, good consistency was found across the subjects. Since the latencies of these effects varied among the subjects, precise determination of directions of shift required within-subject ANOVAs. Also, there existed the possibility that the previously-taken grand ANOVA could have obscured individual differences with opposite directionality. Therefore, we performed the individual comparisons between the areas on the latencies of the significant effects found in the grand ANOVAs. The F_{peak} measure was applied to the individual ANOVAs to identify the latency of effects in

each area (as defined in the section “Statistical analysis of activation shift based on averaged responses”). Representative time courses of F -values are shown in Figure 5 for one subject for the peripheral stimuli at high contrast (A, B), and at low contrast (C). The peak F -values used are indicated by the arrowheads.

Figure 6(A) shows the latencies of all subjects for the effect of vertical position in the early period (40.8–93.6 ms, circles), and in the middle period (104.8–152.8 ms, triangles), in V1/V2 relative to hMT+. The early effect began in V1/V2 and followed in hMT+ in all subjects. This clearly represents a shift. In contrast, the middle period effect in V1/V2 led in only two subjects, implying that the early period effect in V1/V2 and not the middle period, induced the effect in hMT+. The mean and SD of the delay of hMT+ with respect to V1/V2 was 54.8 ± 15.7 ms.

The latencies of the motion effect at high contrast are shown in Figure 6(B) for peripheral (circles) and central

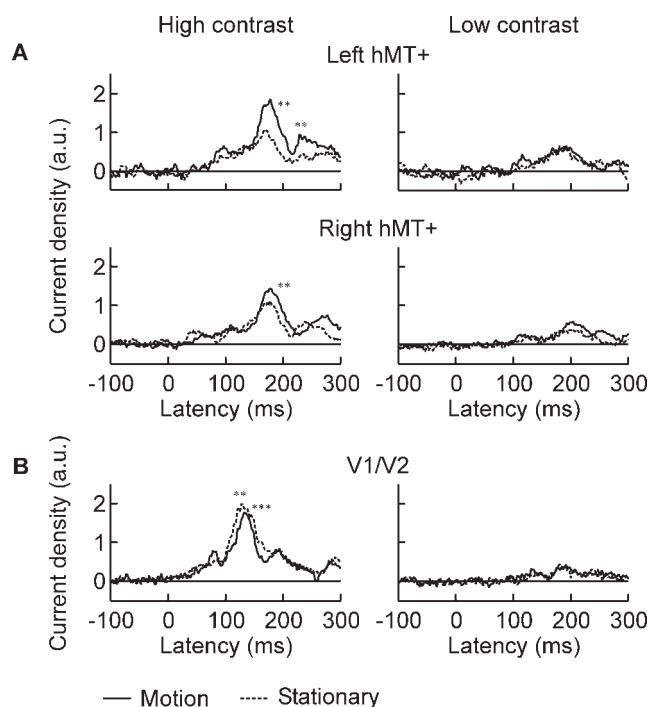


Figure 3.

Grand-averaged responses to central stimuli. **(A)** Responses of hMT+ to motion stimuli (solid lines) and stationary stimuli (dashed lines). **(B)** Responses of V1/V2. Significant effects between the conditions, as revealed by the grand ANOVA are marked by asterisks (**, $P < 0.01$; ***, $P < 0.001$) (see Table 1 for factors considered).

(diamonds) stimuli. The motion effect in V1/V2 was earlier than in hMT+ in all subjects. This is shown by the fact that the means and SDs of the hMT+ delay with respect to V1/V2 for the peripheral and central stimuli were 33.8 ± 18.7 ms and 42.6 ± 20.0 ms, respectively. Finally, Figure 6(C) plots the latencies of the lateralization effect at low contrast. The lateralization effect began in hMT+ and followed in V1/V2 in all subjects, suggesting an activation shift from hMT+ to V1/V2 at low contrast. The mean and SD of the delay was 26.8 ± 19.4 ms.

Results of Mutual Information Analysis Based on Response Variances

Using the peripheral stimuli, we examined the relatedness between V1/V2 and the contralateral hMT+, and between V1/V2 and ipsilateral hMT+. Figure 7 shows results of the MI analysis at representative latencies for which the difference in MI between the two possible directions of relatedness [$MI_{V1 \rightarrow MT}(t, \tau)$ vs. $MI_{MT \rightarrow V1}(t, \tau)$] was largest. In other words, the latencies were chosen so as to maximize the difference between V1/V2 leading hMT+

and the reverse (hMT+ leading V1/V2). For the high-contrast stimuli presented to the lower visual field, an ANOVA revealed that the MI between V1/V2 and contralateral hMT+ was significantly higher when V1/V2 led in MI [left filled bar in Fig. 7(A)] than when hMT+ led (right filled bar) (i , $P < 0.05$). This comparison implies that activation shifted from V1/V2 to hMT+. On the other hand, for the peripheral stimuli at low contrast, the MI between V1/V2 and ipsilateral hMT+ was significantly higher when hMT+ led [right open bar in Fig. 7(C)] than when V1/V2 led (left open bar) (iv , $P < 0.05$), suggesting the reverse direction of shift. At high contrast, we also found that the V1/V2's lead in MI was significantly higher for the bottom than top stimuli [ii in Fig. 7(A), $P < 0.05$], and for the stationary than motion stimuli for presentation in the central visual field [iii in Fig. 7(B), $P < 0.05$].

The latencies of all significant measures of relatedness ranged from 8 to 48 ms and are summarized in Figure 8. For the high-contrast stimuli, significant relatedness was always led by V1/V2 ($P < 0.05$), as plotted above the diagonal dashed line. No significant relatedness led by hMT+ was found at high contrast. In the low-contrast condition, we found significantly stronger relatedness led by ipsilateral hMT+ over V1/V2 for the stimuli presented to the left visual field ($P < 0.05$), as plotted below the diagonal dashed line in green. For the central stimuli, no significant relatedness led by hMT+ was found, nor was any found at low contrast.

Our MI results, therefore, show that the direction of activation shift is always from V1/V2 to hMT+ at high contrast, but sometimes in the opposite direction at low contrast.

Summary of Directions of Activation Shift

The direction of estimated shift in averaged response and in response variance is summarized in Figure 9. The dominant flow of processing was from V1/V2 to hMT+ at high contrast, and from hMT+ to V1/V2 at low contrast. The shifts found according to averaged response usually but not always matched those obtained with MI. For example, the peripheral motion shift estimated by averaged response [M_P in Fig. 9(A)] was not matched by an analogous shift seen with MI. These results show that while largely in agreement, both methods reveal slightly different aspects of activation shift between connected areas.

DISCUSSION

Measuring Activation Shift with MEG

We began by localizing V1/V2 using stationary and motion stimuli, and hMT+ by taking the difference between stationary and motion stimuli. The ROIs defined for V1/V2 were located around the calcarine sulcus as expected, and exhibited retinotopy. The ROIs defined for

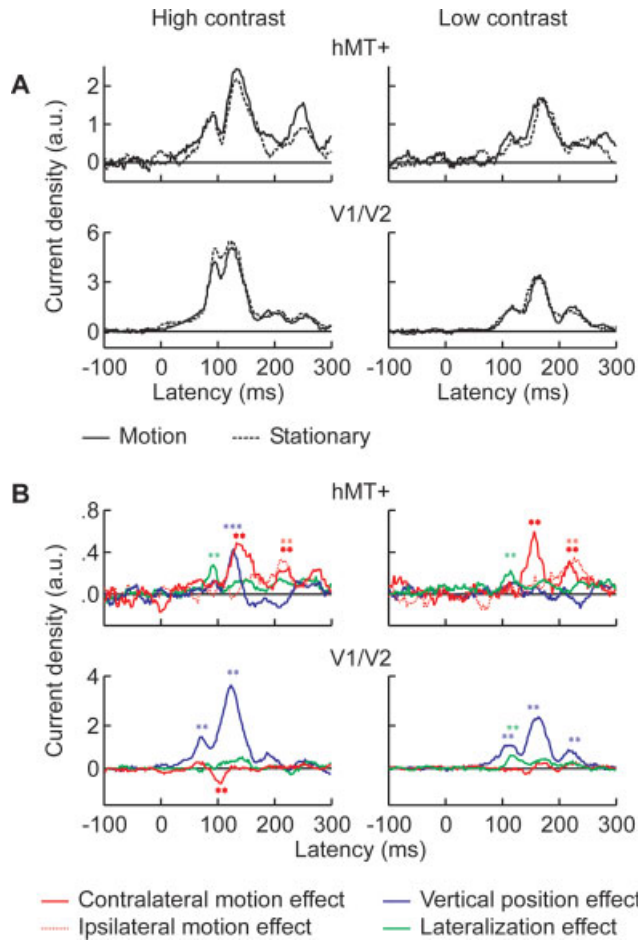


Figure 4.

Grand-averaged response to peripheral stimuli. **(A)** Time course of the response in the left hemisphere to motion stimuli (solid lines) and stationary stimuli (dashed lines) presented to a peripheral location (namely, the lower right visual field). **(B)** Average across peripheral stimuli, taken after subtractions of responses to: stationary stimuli from motion stimuli on the contralateral side (representing the contralateral motion effect, solid red line); stationary from motion stimuli ipsilaterally (dashed red line); the top stimuli from the bottom stimuli (blue line); and of the right hemisphere from the left (green line). The latency of the significant effects revealed by the grand ANOVA is indicated for stimulus motion in the contralateral hemisphere (bold red “***”), and in the ipsilateral hemisphere (thin red “***”). Blue “***” and “***”, significant effects of vertical position. Green “***”, significant effects of lateralization. “***” indicates a significance level of 0.01. “***” indicates a significance level of 0.001.

hMT+ were in agreement with previous fMRI studies [Dumoulin et al., 2000; Hasnain et al., 1998; Tootell et al., 1995] and clustered around the junction of the inferior temporal sulcus with its ascending limb and the lateral occipital sulcus, as expected following Dumoulin et al. [2000].

Our study found that the effect of stimulus conditions on the averaged response began in V1/V2 and followed in hMT+ at high contrast. At high contrast, the relatedness in response variance as determined by MI was led by V1/V2,

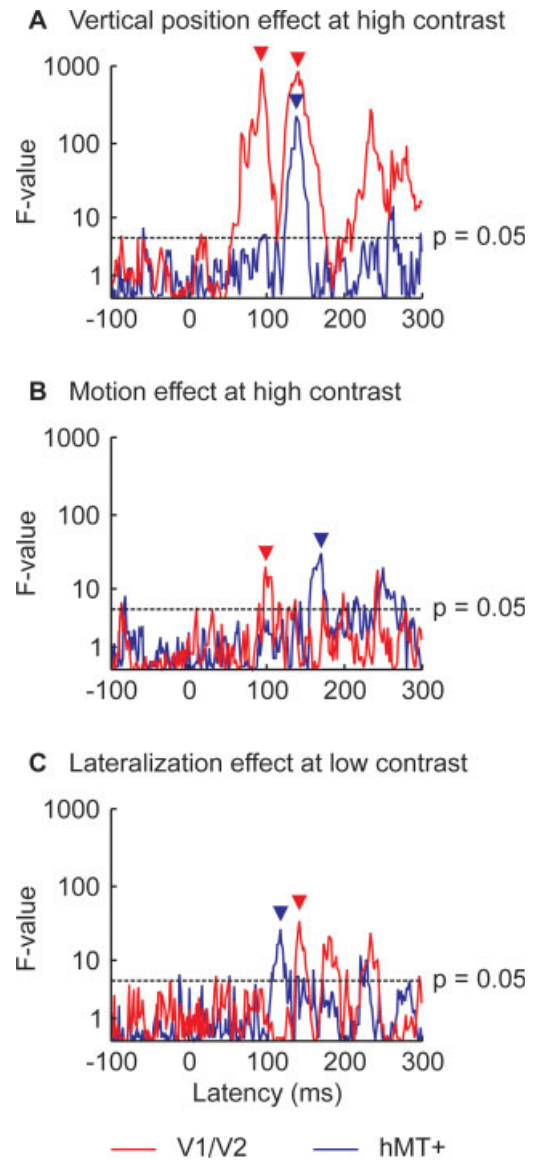


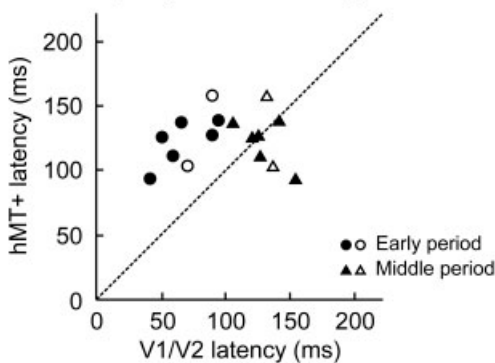
Figure 5.

Time course of F -value in an individual ANOVA in one subject for the peripheral stimuli. Red and blue lines indicate the F -values in V1/V2 and hMT+, respectively. **(A)** Main effect of vertical stimulus position at high contrast. **(B)** Main effect of motion for V1/V2 and the interaction between motion and horizontal stimulus position for hMT+ at high contrast. **(C)** Main effect of lateralization at low contrast. Horizontal dashed lines denote a significance threshold of $P = 0.05$ (i.e., $F_{1,9} = 5.1$). Arrowheads denote the latencies of the peak F -values used to determine the order of effects between V1/V2 and hMT+ for this subject.

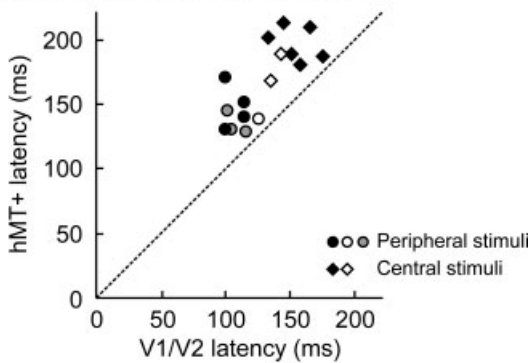
while at low contrast it was led by hMT+. At low contrast, a lateralization effect was first found in hMT+ and later recurred in V1/V2. Putting together these results, we suggest that the direction of activation shift was from V1/V2 to hMT+ at high contrast, but in the reverse direction at low contrast. While there remains a possibility that these effects may have resulted from common inputs from a third area, the evidence on the interaction between V1 and MT in monkey studies [Hupe et al., 1998; Movshon and Newsome, 1996] strongly favors the interpretation that these are the results of direct interaction between these two areas.

In the current study, the activation shift occurred within a range of 8–48 ms, in accordance with TMS studies, which have indicated a range between 5 and 50 ms [Beckers and Zeki, 1995; Pascual-Leone and Walsh, 2001; Silvanto et al., 2005a]. This may appear long in comparison with monkey studies which show that an action potential may travel between V1 and MT within milliseconds through direct connections [Movshon and Newsome, 1996]. However, MEG measures the activation of neuron populations rather than individual neurons [Hamalainen et al., 1993], thus the slower activation shift seen here most likely reflects processing at the population level.

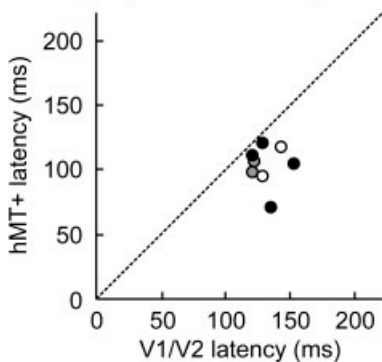
A Vertical position effect at high contrast
(Peripheral stimuli only)



B Motion effect at high contrast



C Lateralization at low contrast
(Peripheral stimuli only)



Activation Shifts as Measured by Averaged Response and by Response Variances

As described earlier, we measured shifts of activation using two methods: by obtaining the latencies in averaged responses between areas, and by measuring the degree of relatedness in the response variances between areas, using Mutual Information Analysis.

It is known that evoked neural responses are determined by both externally applied stimuli and the ongoing brain state [Arieli et al., 1996; Laskaris et al., 2003]. The ongoing state spontaneously fluctuates at low frequencies of less than 0.1 Hz during rest [Fox et al., 2005], and varies from trial to trial in a button-press task [Fox et al., 2006] as revealed by correlation analysis across brain areas. It is also associated with the trial-to-trial variation in subjects' percepts [Ress and Heeger, 2003]. Despite these factors, the variance in evoked response to identical stimuli is often treated as experimental noise.

Our study deliberately took a different approach. We specifically examined the variance across runs for evidence

Figure 6.

Individual subject comparisons of the latency of significant effects between V1/V2 and hMT+, as given by F_{peak} . Each symbol represents one comparison for each subject. Horizontal and vertical axes are taken as response latencies from the onset of the stimulus. Symbols above the diagonal lines imply a shift in direction from V1/V2 to hMT+, while those below imply the reverse direction. In all panels, filled symbols indicate the latency for subjects who significantly exhibited the prevailing effect in both areas. Gray symbols indicate that the effect was significant in just one area. Open symbols indicate the latency for subjects who exhibited the prevailing effect directions in one area and the opposite effect direction in another area. The prevailing effects were as follows: **(A)** A higher response to bottom than top stimuli in both V1/V2 and hMT+ at high contrast (a vertical position effect); **(B)** A higher response to motion than stationary stimuli in hMT+, but a higher response to stationary than motion stimuli in V1/V2 at high contrast (a motion effect); and **(C)** A higher response in the left than right hemisphere in both areas at low contrast (a lateralization effect).

of relatedness between areas. At the same time, we strove to maintain a constant level of arousal by means of a button-press task. Other internal conditions such as attention [Gandhi et al., 1999] and adaptation to the experimental environment, however, were still free to vary. Thus, the relatedness in response variance obtained in the current study should reflect a coupling of these internal states and the applied stimulus.

Recall that we had found a transfer of motion-related activation for the peripheral stimuli based on averaged responses [M_P in Fig. 9(A)]. This was not accompanied by a comparable MI relatedness effect. We believe this discrepancy reveals the difference in focus between the two methods of analysis. Whereas mutual information derived

from response variances is sensitive to background brain states, the analysis of grand-averaged responses cancels these out, revealing a purer signal related to the processing of peripheral motion from V1/V2 to hMT+. However, our method of MI analysis is designed to detect nonlinear effects between stimulus conditions and background brain states. The results indicate that there was no such effect between stimulus motion and background brain states, a finding complementary to the finding based on averaged responses.

Lateralization Effect

The right-handed subjects measured in our study showed significantly higher activation in the left hemisphere in hMT+ for the peripheral visual field [Fig. 4(B), green asterisks]. Stronger relatedness in response variance led by hMT+ over V1/V2 was obtained in the left hemisphere [Fig. 7(C)]. Since one of the main functions of hMT+ is the processing of motion signals, these results may reflect lateralization in motion processing. We also found a left bias in the motion effect in hMT+ for central visual field presentations (Fig. 3). Such biased processing in the left hemisphere might serve a role in the dominant-hand control of our right-handed subjects.

More than 90% of humans show functional dominance of the left hemisphere [Sun and Walsh, 2006]. In a previous PET study, left-hemisphere dominance was reported in the inferior parietal lobe of right-handed subjects during

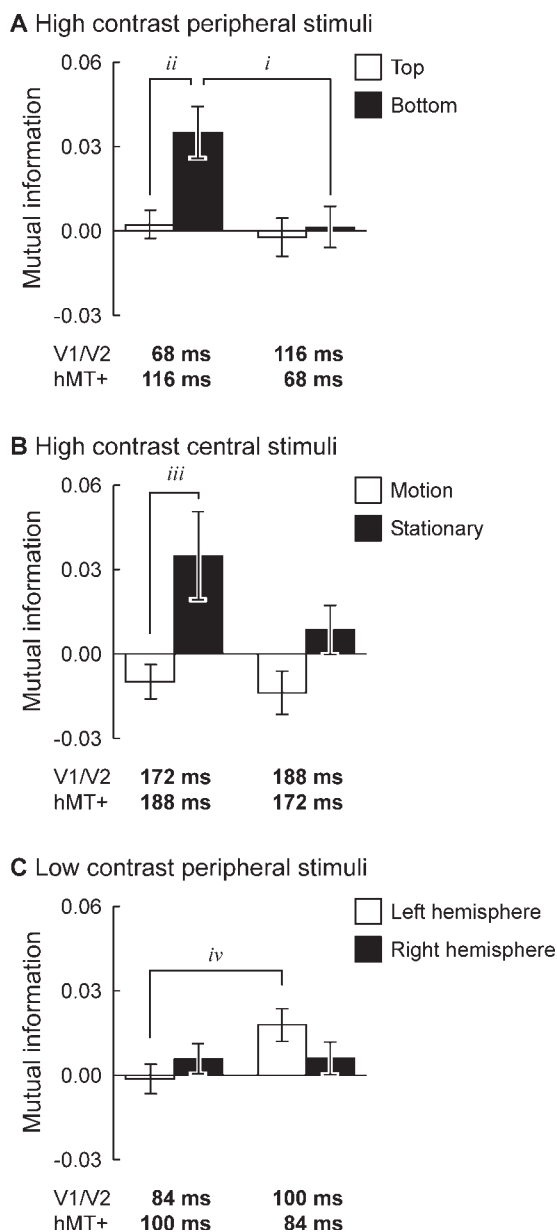


Figure 7.

Results of Mutual Information Analysis. The representative latencies shown at the bottom of each panel are those for which the difference in MI between the orders [$MI_{V1 \rightarrow MT}(t, \tau)$ vs. $MI_{MT \rightarrow V1}(t, \tau)$] was largest. In other words, the latencies were chosen so as to maximize the difference between V1/V2 leading hMT+ (left pairs of bars) and the reverse (hMT+ leading V1/V2; right pairs of bars). When V1/V2's latency is shorter than that of hMT+, we termed it "V1/V2 leading" (left bars). The reverse situation is shown in the right bars. (A) MI measure comparison between V1/V2 leading and contralateral hMT+ leading, in the case of high contrast peripheral stimuli presented to the upper or lower visual field. (B) MI measure comparison as in (A), in this case between V1/V2 leading and left hMT+ leading for high contrast central stimuli. (C) MI measure comparison as in (A), in this case between V1/V2 and ipsilateral hMT+ for low contrast peripheral stimuli. *i*. Relatedness was significantly led by V1/V2 over hMT+ for bottom stimuli. *ii*. Relatedness led by V1/V2 was significantly higher for the bottom than top stimuli. *iii*. Relatedness led by V1/V2 was significantly higher for the stationary than motion stimuli. *iv*. Relatedness was significantly led by hMT+ over V1/V2 for left stimuli. Note: Negative MI values may occur since in our correction process we subtract the MI values obtained from randomized samples from the MI value obtained from the original samples (see Appendix for details).

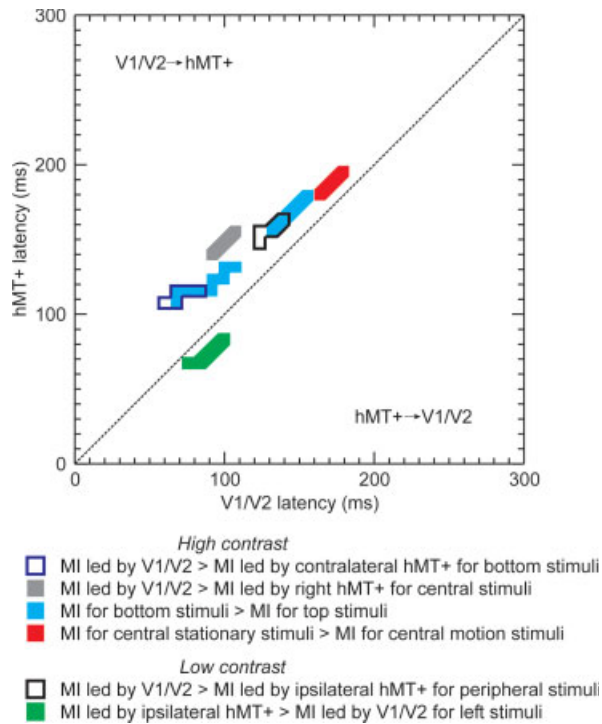


Figure 8.

Latency map of significant relatedness in response variances between V1/V2 and hMT+, as quantified by Mutual Information Analysis. Horizontal and vertical axes are taken as latencies of V1/V2 and hMT+ from the onset of the stimulus. The area above the diagonal dashed line represents relatedness led by V1/V2 (V1/V2→hMT+), while the area below represents hMT+ leading, (i.e. hMT+→V1/V2). Solid cyan areas denote stronger relatedness for bottom versus top stimuli, between V1/V2 and contralateral hMT+. Red areas indicate greater relatedness for central stationary than motion stimuli, between V1/V2 and left hMT+. Other areas are as noted in the legend. Note that for all high contrast stimuli V1/V2 responses lead hMT+ responses, and the only responses for which hMT+ leads, are those to low contrast stimuli on the ipsilateral side.

speed discrimination of motion stimuli [Corbetta et al., 1991]. Conversely, TMS applied to the left hMT+ impaired detection of motion direction much more than to the right hMT+ [Kubova et al., 1990] (however, see [Nakamura et al., 2003] for contrasting results). Overall, the current study lends further support to left hemisphere dominance in early visual processing.

It has been shown that ipsilateral activation to hemifield motion stimulation is delayed in left hMT+ compared with right [ffytche et al., 2000]. These authors also show a 3 ms transfer delay from left to right hMT+, but a 10 ms delay from right to left, suggesting a natural asymmetry in activation between the two hemispheres. While at first glance this may appear as a confound to our results, we argue that such a bias would increase the delays in left

hemisphere activation, but could not explain the lateralization effect found. If the lateralization in left hMT+ were the result of cross-callosal input from right hMT+ the lateralization effect should be expected to appear first in the right hemisphere. However, this is not seen in our results.

Another possibility is that the existence of common input to hMT+ and V1/V2 (such as LGN) could have induced the lateralization effect. However, we note that the lateralization effect appeared in both V1/V2 and hMT+ at low contrast, but only in hMT+ at high contrast [Fig. 4(B), green asterisks]. If a common source such as LGN were responsible, the lateralization effect should appear both in V1/V2 and hMT+, or in neither area. Since this was not the case at high contrast (with the lateralization effect appearing first in hMT+ and then in V1/V2), a more plausible explanation is that the effect shifted from hMT+ to V1/V2.

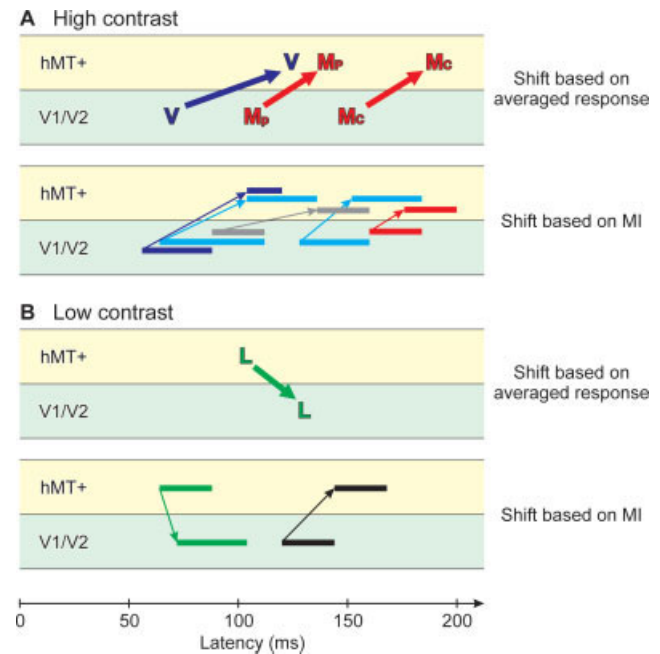


Figure 9.

Summary of activation shifts from V1/V2 to hMT+ at high contrast (A), and from hMT+ to V1/V2 at low contrast (B). Latencies for estimated shift in averaged response are given by the horizontal position of the boldface abbreviations. Latencies for the estimated shift in response variances are indicated by the horizontal bars, and show a similar trend to the shift in averaged response. Bar length reflects the duration over which Mutual Information value was significant. The abbreviations indicate the latencies of: Lateralization effect (L); Vertical position effect (V); Motion effect (peripheral, M_p ; central, M_c). Pairs of horizontal bars connected by thin arrows indicate the latencies for periods of significant relatedness in response variance between V1/V2 and hMT+, as revealed by Mutual Information Analysis. For a description of relatedness indicated by color, see the legend to Figure 8.

Responses to Motion Stimuli in hMT+ and V1/V2

When the stimuli were presented to the peripheral visual field, we obtained significant motion effects in hMT+ in two periods: 135–160 ms, and 210–230 ms [Fig. 4(B), bold and thin red asterisks]. These early and late motion effects were obtained in the contralateral hemisphere and in bilateral hemispheres, respectively. With centrally presented stimuli, bilateral responses were obtained at a latency of 196.0 ms. It is known that hMT+ consists of two sub-regions: the middle temporal area (MT) [Huk et al., 2002] which is believed to project to the medial superior temporal area (MST). The receptive fields of MT neurons are restricted to contralateral input while MST neurons receive input from the ipsilateral field as well. This has been found both in monkeys [Albright and Desimone, 1987; Komatsu and Wurtz, 1988; Tanaka and Saito, 1989] and in humans [Huk et al., 2002]. These anatomical facts, together with our findings of dual latencies are consistent with a model in which MT first receives visual inputs which are later integrated by MST.

In contrast to hMT+, we found significantly higher activation in V1/V2 for the stationary stimuli than the motion stimuli at high contrast [Figs. 3(A) and 4(A)]. Previous fMRI [Chawla et al., 1999; Tootell et al., 1995] and PET [Zeki et al., 1991] studies in V1 obtained either similar or higher activation for moving stimuli compared with stationary stimuli when these were large (>14 deg). Conversely, Sunaert et al. [1999] obtained stronger activation for stationary stimuli when the stimuli they presented were small (3 deg), high contrast (0.97), and directed to the central visual field. Considering the similarly small size of our central stimuli (2 deg), our results agree with these studies and suggest a dependence of the motion effect on stimulus size.

Advantage of the Lower Visual Field

Higher responses to the bottom versus top stimuli were obtained in V1/V2 at both luminance contrasts [Fig. 4(B), blue asterisks], consistent with the advantage of the lower visual field found in previous MEG studies using high contrast checkerboards [Portin et al., 1999], vertical gratings [Tzelepi et al., 2001], and face stimuli [Liu and Ioannides, 2006], as well as an fMRI study which also used checkerboard stimuli [Chen et al., 2004]. After adjusting spatial luminance uniformity (see Materials and Methods), we confirmed the lower visual field advantage and extended upon the earlier findings for motion stimuli. In addition, we revealed higher responses in hMT+ [Fig. 4(B), blue asterisks] and greater relatedness in the response variance between V1/V2 and hMT+ [Fig. 7(A)] for the bottom than top stimuli at high contrast. It is worth noting that in humans, rod density on the superior retina (representing the lower visual field) is higher than in the inferior retina [Curcio et al., 1990]. The advantage of the lower visual field in V1/V2 might originate from this retinal asym-

metry, and persist on to higher visual areas such as hMT+ at high contrast.

Functional Role of Activation Shift from hMT+ to V1/V2

Our finding of a lateralization effect in which hMT+'s activity preceded that of V1/V2 at low contrast suggests that MT compensates for weak motion signals arriving from V1. MT is known to have much larger receptive fields than V1. In the monkey, V1 receptive fields range somewhat below 0.5 degrees, while MT receptive fields range between 6 and 10 degrees [Qian and Andersen, 1994]. In humans, these receptive field sizes have been estimated at less than 2 degrees for V1 and around 8.4 degrees or greater for MT [Yoshor et al., 2007], consistent with the monkey data. In monkeys, surround modulation of MT receptive field has been found to expand spatially as a result of decreasing the luminance contrast of a field of moving dots [Pack et al., 2005]. Therefore, it seems reasonable that MT neurons are better able than V1 neurons to sum weak signals at low contrast. In this case, the integrative ability of MT should produce at least partial resolution of motion direction despite weak stimulation of V1. In humans, activation in V1 dramatically drops as stimulus contrast decreases, but hMT+'s response to motion stimuli is less sensitive to such a decrease in contrast [Tootell et al., 1995]. As is found in the interaction between V1 and LGN [Sillito et al., 2006], feedback from MT to V1 would thus be able to enhance coherent input consistent with the motion direction integrated in MT. Taken together, our results suggest that since hMT+ receptive fields are larger, they may be better able to collect weak signals from V1/V2, such as those present in a low contrast stimulus, integrate them, and enhance V1/V2 representations through feedback.

ACKNOWLEDGMENTS

We thank Mr. K. Haruhana for valuable technical assistance in data recording and Ms. Y. Okazaki for collaborative work on the installation of the projector as well as generous advice on the experiment.

REFERENCES

- Albright TD, Desimone R (1987): Local precision of visuotopic organization in the middle temporal area (MT) of the Macaque. *Exp Brain Res* 65:582–592.
- Andersen RA, Bradley DC (1998): Perception of three-dimensional structure from motion. *Trends Cognit Sci* 2:222–228.
- Arieli A, Sterkin A, Grinvald A, Aertsen A (1996): Dynamics of ongoing activity: Explanation of the large variability in evoked cortical responses. *Science* 273:1868–1871.
- Beckers G, Zeki S (1995): The consequences of inactivating areas V1 and V5 on visual motion perception. *Brain* 118 (Part 1):49–60.

- Born RT, Bradley DC (2005): Structure and function of visual area MT. *Ann Rev Neurosci* 28:157–189.
- Chawla D, Buechel C, Edwards R, Howseman A, Josephs O, Ashburner J, Friston KJ (1999): Speed-dependent responses in V5: A replication study. *Neuroimage* 9:508–515.
- Chen H, Yao D, Liu Z (2004): A study on asymmetry of spatial visual field by analysis of the fMRI BOLD response. *Brain Topogr* 17:39–46.
- Cheng K, Fujita H, Kanno I, Miura S, Tanaka K (1995): Human cortical regions activated by wide-field visual-motion—An (H₂O)-O-15 pet study. *J Neurophysiol* 74:413–427.
- Corbetta M, Miezin FM, Dobmeyer S, Shulman GL, Petersen SE (1991): Selective and divided attention during visual discriminations of shape, color, and speed—Functional-anatomy by positron emission tomography. *J Neurosci* 11:2383–2402.
- Curcio CA, Sloan KR, Kalina RE, Hendrickson AE (1990): Human photoreceptor topography. *J Compar Neurol* 292:497–523.
- Dumoulin SO, Bittar RG, Kabani NJ, Baker CL, Le Goualher G, Pike GB, Evans AC (2000): A new anatomical landmark for reliable identification of human area V5/MT: A quantitative analysis of sulcal patterning. *Cerebral Cortex* 10:454–463.
- ffytche DH, Howseman A, Edwards R, Sandeman DR, Zeki S (2000): Human area V5 and motion in the ipsilateral visual field. *Eur J Neurosci* 12:3015–3025.
- Fox MD, Snyder AZ, Vincent JL, Corbetta M, van Essen DC, Raichle ME (2005): The human brain is intrinsically organized into dynamic, anticorrelated functional networks. *Proc Natl Acad Sci USA* 102:9673–9678.
- Fox MD, Snyder AZ, Zacks JM, Raichle ME (2006): Coherent spontaneous activity accounts for trial-to-trial variability in human evoked brain responses. *Nat Neurosci* 9:23–25.
- Foxe JJ, Simpson GV (2002): Flow of activation from V1 to frontal cortex in humans. A framework for defining “early” visual processing. *Exp Brain Res* 142:139–150.
- Gandhi SP, Heeger DJ, Boynton GM (1999): Spatial attention affects brain activity in human primary visual cortex. *Proc Natl Acad Sci USA* 96:3314–3319.
- Girard P, Salin PA, Bullier J (1992): Response selectivity of neurons in area-Mt of the Macaque monkey during reversible inactivation of area-V1. *J Neurophysiol* 67:1437–1446.
- Grynszpan F, Geselowitz DB (1973): Model studies of the magnetocardiogram. *Biophys J* 13:911–925.
- Hamalainen M, Hari R, Ilmoniemi RJ, Knuutila J, Lounasmaa OV (1993): Magnetoencephalography—Theory, instrumentation, and applications to noninvasive studies of the working human brain. *Rev Mod Phys* 65:413–497.
- Hasnain MK, Fox PT, Woldorff MG (1998): Intersubject variability of functional areas in the human visual cortex. *Human Brain Map* 6:301–315.
- Hironaga N, Schellens M, Ioannides AA (2002): Accurate co-registration for MEG reconstructions. In: Nowak H, Hueisen J, Giesler F, Huonker R, editors. *Proceedings of the 13th International Conference on Biomagnetism*. VDE Verlag, Berlin, Jena. pp 931–933.
- Huk AC, Dougherty RF, Heeger DJ (2002): Retinotopy and functional subdivision of human areas MT and MST. *J Neurosci* 22:7195–7205.
- Hupe JM, James AC, Payne BR, Lomber SG, Girard P, Bullier J (1998): Cortical feedback improves discrimination between figure and background by V1, V2 and V3 neurons. *Nature* 394:784–787.
- Inui K, Kakigi R (2006): Temporal analysis of the flow from V1 to the extrastriate cortex in humans. *J Neurophysiol* 96:775–784.
- Ioannides A.A., (1994): Estimates of brain activity using magnetic field tomography and large scale communication within the brain. *Bioelectrodyn Biocommun*. Singapore: World Scientific. pp 319–353.
- Ioannides AA (1995): Estimates of 3D brain activity ms by ms from biomagnetic signals: Method (MFT), results and their significance. In: Eiselt E, Zwiener U, Witte H, editors. *Quantitative and Topological EEG and MEG Analysis*. Jena: Universitätsverlag Druckhaus-Maayer. pp 59–68.
- Ioannides AA. 2002: Magnetic field tomography: Theory, applications and examples from the visual system. In: Hirata K., Kotani M, Koga Y, Nagata K, Yamazaki K, editors. *Recent Advances in Human Brain Mapping*. Amsterdam, Elsevier. *Int Congress Ser* 1232:261–270.
- Ioannides AA, Bolton JPR, Clarke CJS (1990): Continuous probabilistic solutions to the biomagnetic inverse problem. *Inverse Problems* 6:523–542.
- Jahn O, Cichocki A, Ioannides AA, Amari S (1999): Identification and elimination of artifacts from MEG signals using extended independent component analysis. In: Yoshimoto T, Kotani M, Kuriki S, Karibe H, Nakasato N, editors. *Sendai: Tohoku University*. pp 224–228.
- Kapadia MK, Westheimer G, Gilbert CD (1999): Dynamics of spatial summation in primary visual cortex of alert monkeys. *Proc Natl Acad Sci USA* 96:12073–12078.
- Komatsu H, Wurtz RH (1988): Relation of cortical areas Mt and Mst to pursuit eye-movements, Part 1: Localization and visual properties of neurons. *J Neurophysiol* 60:580–603.
- Kubova Z, Kuba M, Hubacek J, Vit F (1990): Properties of visual evoked potentials to onset of movement on a television screen. *Doc Ophthalmol* 75:67–72.
- Laskaris NA, Ioannides AA (2002): Semantic geodesic maps: A unifying geometrical approach for studying the structure and dynamics of single trial evoked responses. *Clin Neurophysiol* 113:1209–1226.
- Laskaris NA, Liu LC, Ioannides AA (2003): Single-trial variability in early visual neuromagnetic responses: An explorative study based on the regional activation contributing to the N70m peak. *Neuroimage* 20:765–783.
- Levitt JB, Lund JS (1997): Contrast dependence of contextual effects in primate visual cortex. *Nature* 387:73–76.
- Liu L, Ioannides AA (2006): Spatiotemporal dynamics and connectivity pattern differences between centrally and peripherally presented faces. *Neuroimage* 31:1726–1740.
- Maunsell JHR, van Essen DC (1983): The connections of the middle temporal visual area (MT) and their relationship to a cortical hierarchy in the Macaque monkey. *J Neurosci* 3:2563–2586.
- Movshon JA, Newsome WT (1996): Visual response properties of striate cortical neurons projecting to area MT in Macaque monkeys. *J Neurosci* 16:7733–7741.
- Nakamura H, Kashii S, Nagamine T, Matsui Y, Hashimoto T, Honda Y, Shibasaki H (2003): Human V5 demonstrated by magnetoencephalography using random dot kinematograms of different coherence levels. *Neurosci Res* 46:423–433.
- Oldfield RC (1971): Assessment and analysis of handedness—Edinburgh inventory. *Neuropsychologia* 9:97–113.
- Pack CC, Hunter JN, Born RT (2005): Contrast dependence of suppressive influences in cortical area MT of alert Macaque. *J Neurophysiol* 93:1809–1815.
- Pascual-Leone A, Walsh V (2001): Fast backprojections from the motion to the primary visual area necessary for visual awareness. *Science* 292:510–512.
- Portin K, Vanni S, Virsu V, Hari R (1999): Stronger occipital cortical activation to lower than upper visual field stimuli—Neuromagnetic recordings. *Exp Brain Res* 124:287–294.
- Qian N, Andersen RA (1994): Transparent motion perception as detection of unbalanced motion signals. II. Physiology. *J Neurosci* 14:7367–7380.

- Ress D, Heeger DJ (2003): Neuronal correlates of perception in early visual cortex. *Nat Neurosci* 6:414–420.
- Rovamo J, Virsu V (1979): An estimation and application of the human cortical magnification factor. *Exp Brain Res* 37:495–510.
- Sceniak MP, Ringach DL, Hawken MJ, Shapley R (1999): Contrast's effect on spatial summation by Macaque V1 neurons. *Nat Neurosci* 2:733–739.
- Schmolesky MT, Wang Y, Hanes DP, Thompson KG, Leutgeb S, Schall JD, Leventhal AG (1998): Signal timing across the Macaque visual system. *J Neurophysiol* 79:3272–3278.
- Shannon CE (1948): The mathematical theory of communication. *Bell Syst Techn J* 27:379–423.
- Sillito AM, Cudeiro J, Jones HE (2006): Always returning: Feedback and sensory processing in visual cortex and thalamus. *Trends Neurosci* 29:307–316.
- Silvanto J, Cowey A, Lavie N, Walsh V (2005a): Striate cortex (V1) activity gates awareness of motion. *Nat Neurosci* 8:143–144.
- Silvanto J, Lavie N, Walsh V (2005b): Double dissociation of V1 and V5/MT activity in visual awareness. *Cerebral Cortex* 15:1736–1741.
- Snowden RJ, Treue S, Erickson RG, Andersen RA (1991): The response of area Mt and V1 neurons to transparent motion. *J Neurosci* 11:2768–2785.
- Sun T, Walsh CA (2006): Molecular approaches to brain asymmetry and handedness. *Nat Rev Neurosci* 7:655–662.
- Sunaert S, Van Hecke P, Marchal G, Orban GA (1999): Motion-responsive regions of the human brain. *Exp Brain Res* 127:355–370.
- Talairach J, Tournoux P (1988). *Co-planar Stereotaxic Atlas of the Human Brain*. New York: Thieme.
- Tanaka K, Saito HA (1989): Analysis of motion of the visual-field by direction, expansion contraction, and rotation cells clustered in the dorsal part of the medial superior temporal area of the Macaque monkey. *J Neurophysiol* 62:626–641.
- Taylor JG, Ioannides AA, Muller-Gartner HW (1999): Mathematical analysis of lead field expansions. *IEEE Trans Med Imaging* 18:151–163.
- Tootell RBH, Reppas JB, Kwong KK, Malach R, Born RT, Brady TJ, Rosen BR, Belliveau JW (1995): Functional-analysis of human Mt and related visual cortical areas using magnetic-resonance-imaging. *J Neurosci* 15:3215–3230.
- Treves A, Panzeri S (1995): The upward bias in measures of information derived from limited data samples. *Neural Comput* 7:399–407.
- Tzelepi A, Ioannides AA, Poghosyan V (2001): Early (N70m) neuromagnetic signal topography and striate and extrastriate generators following pattern onset quadrant stimulation. *Neuroimage* 13:702–718.
- Vrba J, Robinson SE (2001): Signal processing in magnetoencephalography. *Methods* 25:249–271.
- Yoshor D, Bosking WH, Ghose GM, Maunsell JH (2007): Receptive fields in human visual cortex mapped with surface electrodes. *Cereb Cortex* 17:2293–2302.
- Zeki S, Watson JDG, Lueck CJ, Friston KJ, Kennard C, Frackowiak RSJ (1991): A direct demonstration of functional specialization in human visual-cortex. *J Neurosci* 11:641–649.

APPENDIX

Mutual Information Analysis

The key measurement in Mutual Information (MI) Analysis is entropy. The entropy of events in a brain region (R)

within an interval $[t - hw, t + hw]$ (hw: half window size) is defined as:

$$H_{R(t)} = - \sum_{i=1}^{N_R} p_{R(t)}(i) \ln p_{R(t)}(i),$$

where N_R is the number of possible states of the region, and $p_R(i)$ is the probability that the region will be in state i within that interval. The entropy of joint events in two regions (R1, R2) is

$$H_{R1(t),R2(t+\tau)} = - \sum_{i=1}^{N_{R1}} \sum_{j=1}^{N_{R2}} p_{R1(t),R2(t+\tau)}(i,j) \ln p_{R1(t),R2(t+\tau)}(i,j),$$

where $p_{R1(t),R2(t+\tau)}(i,j)$ is the joint probability that R1 will be in state i during the interval, and R2 will be in state j with a delay τ (>0) relative to R1. MI quantifies the relatedness between the two regions' states as:

$$MI_{R1 \rightarrow R2}(t, \tau) = H_{R1(t)} + H_{R2(t+\tau)} - H_{R1(t),R2(t+\tau)}.$$

The value of MI increases as the degree of the relatedness increases. However, MI analysis cannot *irrefutably* distinguish actual interactions between R1 and R2 as opposed to common inputs from a third region.

MI was calculated between V1/V2 and hMT+ ($MI_{V1 \rightarrow MT}$, $MI_{MT \rightarrow V1}$) in each hemisphere, separately for each stimulus condition and for each subject. The state of each ROI was defined as the projection of the current density vector for each run onto the optimal current density direction of that time slice computed by averaging across all runs. The half-window size of the interval was set to 16 ms. 210 samples within the interval and over all runs ($= 21 \times 10$) were used to obtain each MI value. The range of the current density of each region was then defined as the range between the maximum and minimum activations among all runs in each stimulus condition. This range was then divided into 10 intervals (i.e., $N_{R1} = N_{R2} = 10$), and the frequency of samples within each interval was used as the probability. MI was calculated in 8 ms steps in the latency range from -100 to 300 ms and with a range of delays from 8 to 96 ms.

Sometimes MI analysis overestimates relatedness because sample size tends to be limited in practical experiments [Treves and Panzeri, 1995]. Therefore, we randomized the pairs of samples between V1/V2 and hMT+ over the runs and calculated MI as described earlier to obtain a measure of overestimation. We repeated this process over 100 times. The MI values obtained from the randomized samples was averaged and subtracted from the MI values obtained from the original samples. In this article, we use the term MI to refer to the value obtained after this correction by subtraction of the overestimation.